

Hydrogen-bonded systems between monocarboxylic acids and the trinuclear cluster cation $[\text{H}_3\text{Ru}_3(\text{C}_6\text{H}_6)(\text{C}_6\text{Me}_6)_2(\text{O})]^+$: cold-spray ionisation mass spectroscopic and X-ray crystallographic studies

Bruno Therrien ^{a,*}, Ludovic Vieille-Petit ^a, Georg Süss-Fink ^a,
Yoshihisa Sei ^b, Kentaro Yamaguchi ^b

^a Institut de Chimie, Université de Neuchâtel, Case postale 2, CH-2007 Neuchâtel, Switzerland

^b Laboratory of Analytical Chemistry, Tokushima Bunri University, Shido, Sanuki-city, Kagawa 769-2193, Japan

Received 21 April 2004; accepted 9 June 2004

Available online 15 July 2004

Abstract

The hydrogen-bonded systems formed between monocarboxylic acid derivatives and the trinuclear arene-ruthenium cluster cation $[\text{H}_3\text{Ru}_3(\text{C}_6\text{H}_6)(\text{C}_6\text{Me}_6)_2(\text{O})]^+$ (**1**) have been studied in solution by cold-spray ionisation mass spectroscopy (CSI-MS) and in the solid state by single-crystal X-ray structure analysis of the tetrafluoroborate salts. The presence of 1:1 (acid:cluster) adducts in acetone solution has been clearly demonstrated by CSI-MS. Single-crystal X-ray structure analyses of selected acid-cluster complexes show that in every case the hydroxyl of the acid function interacts strongly with the μ_3 -oxo ligand of cation **1**, the O...O distance ranging from 2.499(9) to 2.595(11) Å.

© 2004 Elsevier B.V. All rights reserved.

Keywords: Arene ligands; Cluster complexes; Hydrogen bonds; Ruthenium; Mass spectroscopy

1. Introduction

Cold-spray ionisation mass spectroscopy (CSI-MS) has been used to investigate the solution structure of primary biomolecules [1], labile organic species [2], asymmetric catalysts [3], and supramolecules [4]. The method allows the rapid and precise characterisation of compounds possessing non-covalent interactions such as hydrogen-bonds.

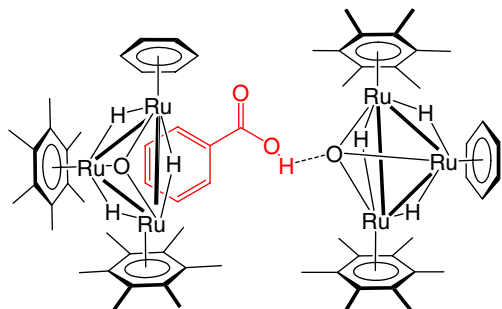
Recently, we have shown the μ_3 -oxo-capped cluster cation $[\text{H}_3\text{Ru}_3(\text{C}_6\text{H}_6)(\text{C}_6\text{Me}_6)_2(\text{O})]^+$ (**1**) to possess inter-

esting host–guest properties [5–7]. Single-crystal X-ray structure analyses show that the μ_3 -oxo ligand is a strong acceptor to form hydrogen bonds, and that the hydrophobic pocket spanned by the three arene ligands acts as a bowl to host different molecules in the solid state. For example, in the presence of benzoic acid, the phenyl group is incorporated in the hydrophobic pocket of the cluster, whereas the hydroxyl group of the acid function is hydrogen-bonded to the μ_3 -oxo ligand of a neighbouring molecule [7], see Scheme 1. However, little is known if such interactions remain in solution.

Therefore, we were interested to investigate the binding properties of **1** in solution with various monocarboxylic acids by CSI-MS. In order to confirm μ_3 -oxo...acid hydrogen bonding, single-crystal X-ray structure

* Corresponding author.

E-mail address: bruno.therrien@unine.ch (B. Therrien).



Scheme 1.

analyses of selected acid-cluster complexes have been performed.

2. Results and discussion

The trinuclear cluster $[\text{H}_3\text{Ru}_3(\text{C}_6\text{H}_6)(\text{C}_6\text{Me}_6)_2(\text{O})]^+$ (**1**) is accessible in aqueous solution from the dinuclear precursor $[\text{H}_3\text{Ru}_2(\text{C}_6\text{Me}_6)_2]^+$ and the mononuclear building block $[\text{Ru}(\text{C}_6\text{H}_6)(\text{H}_2\text{O})_3]^{2+}$ [5]. The tetrafluoroborate salt of **1** is well soluble in acetone, dimethylsulfoxide, dichloromethane and ethanol, and sparingly soluble in water, methanol and chloroform. The μ_3 -oxo ligand is capable of forming hydrogen bonds with donor molecules as observed in the crystal structures of $[\mathbf{1}][\text{BF}_4] \cdot \text{H}_2\text{O}$ [5], $[\mathbf{1}][\text{BF}_4] \cdot \text{H}_2\text{O} \cdot 0.5 \text{ C}_4\text{H}_8\text{O}_2$, $[\mathbf{1}][\text{BF}_4] \cdot \text{H}_2\text{O} \cdot \text{C}_6\text{H}_5\text{OH}$, and $[\text{C}_6\text{H}_5\text{COOH} \subset \mathbf{1}][\text{BF}_4]$ [7]. However, in solution, the only evidence for interactions between the complex and guest molecules was an electrospray ionisation mass spectrometric study which showed **1** to form an adduct with a benzene molecule [8]. By NMR spectroscopy no interaction could be observed between **1** and benzoic acid, even at low temperature, the signals of the benzoic acid remaining unchanged in the presence of **1** [9]. Therefore, we were interested to investigate the presence of hydrogen bond interactions in solution by CSI-MS. We carried out a series of CSI-MS measurements of mixture of monocarboxylic acids with $[\mathbf{1}][\text{BF}_4]$ in acetone.

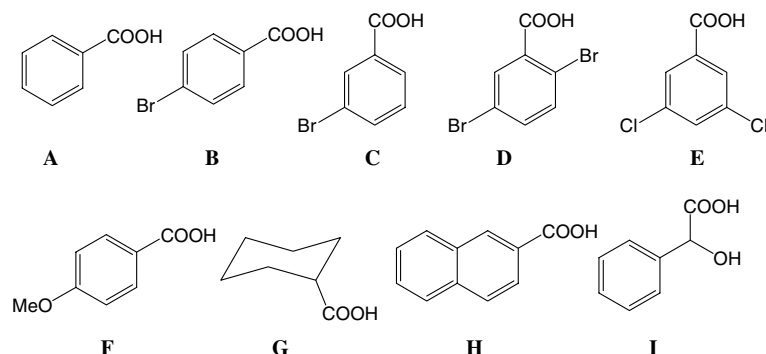
The monocarboxylic acid derivatives used for the present study are presented in Scheme 2; benzoic acid (**A**), 4-bromobenzoic acid (**B**), 3-bromobenzoic acid (**C**), 2,5-dibromobenzoic acid (**D**), 3,5-dichlorobenzoic acid (**E**), 4-methoxybenzoic acid (**F**), cyclohexanecarboxylic acid (**G**), 2-naphtioic acid (**H**) and mandelic acid (**I**).

2.1. Cold-spray ionisation mass spectroscopy

In order to optimise the signal of the ion peak of the adduct products, we first measured in the full mass range a 10:1 mixture of **B** and $[\mathbf{1}][\text{BF}_4]$ in different solvents such as acetone, chloroform, dichloromethane and methanol. The strongest $[\mathbf{1} + \mathbf{B}]^+ / [\mathbf{1}]^+$ signal ratio was found in acetone, whereas no adduct signal was detected in methanol and only a very weak one in dichloromethane. Interestingly, in chloroform a peak at m/z 845 was observed, corresponding to a $[\mathbf{1} + \text{CHCl}_3]^+$ system. This result is in agreement with the fact that crystallisation of $[\mathbf{1}][\text{BF}_4]$ in a mixed acetone–chloroform solution gives the host–guest complex as the tetrafluoroborate salt $[\text{CHCl}_3 \subset \mathbf{1}][\text{BF}_4]$ [7]. Therefore, we can assume that the same weak interactions by means of which the chloroform molecule is hosted in the hydrophobic pocket of **1**, found in the solid state, persist also in solution.

In a typical experiment, 1 μmol of $[\mathbf{1}][\text{BF}_4]$ was dissolved in acetone (3 mL) with 10 μmol of the acid, after complete dissolution of the products, the solution was injected at -20°C by syringe pump in the cold-spray ion source. The mass spectrum measurements were performed with a sector (BE) mass spectrometer (JMS-700, JEOL) equipped with a CSI source.

In all cases a major peak at m/z 725 corresponding to $[\text{H}_3\text{Ru}_3(\text{C}_6\text{H}_6)(\text{C}_6\text{Me}_6)_2(\text{O})]^+$ was observed. The adducts $[\mathbf{1} + \mathbf{B}]^+$, $[\mathbf{1} + \mathbf{C}]^+$, $[\mathbf{1} + \mathbf{D}]^+$, $[\mathbf{1} + \mathbf{E}]^+$, $[\mathbf{1} + \mathbf{F}]^+$, $[\mathbf{1} + \mathbf{H}]^+$ and $[\mathbf{1} + \mathbf{I}]^+$ have been clearly identified in the CSI-MS spectrum. The peaks have been assigned unambiguously on the basis of their characteristic Ru_3 isotope pattern. The $[\mathbf{1} + \text{acid}]^+$ spectra are presented in Fig. 1.



Scheme 2.

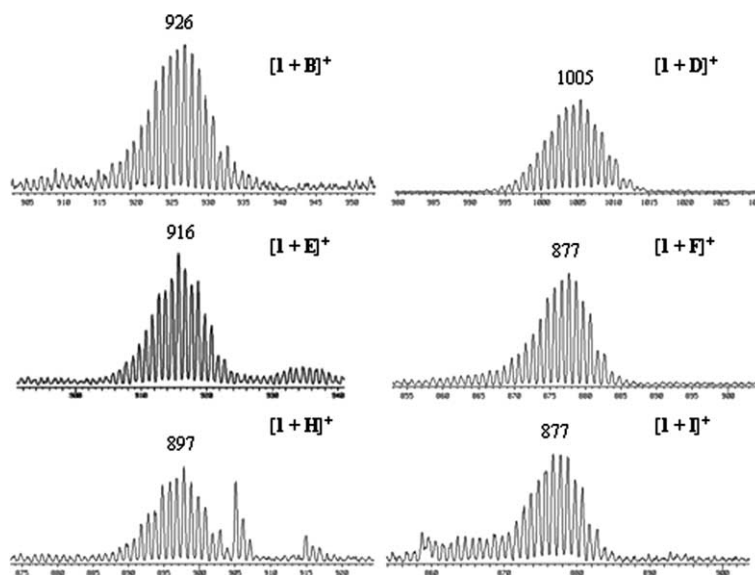


Fig. 1. CSI-MS spectrum of $[1 + \mathbf{B}]^+$, $[1 + \mathbf{D}]^+$, $[1 + \mathbf{E}]^+$, $[1 + \mathbf{F}]^+$, $[1 + \mathbf{H}]^+$, and $[1 + \mathbf{I}]^+$ in acetone solution.

Surprisingly, no adduct of **1** was observed with benzoic acid (**A**) and cyclohexanecarboxylic acid (**G**), even upon increasing the acid concentration. However, in the mass spectrum of $[1]^+$ with 4-bromobenzoic acid (**B**) and 3-bromobenzoic acid (**C**), signals at m/z 926, corresponding to the $[1 + \text{acid}]^+$ adducts were observed. Under the conditions used, it seems that the bromine position has no particular effect on the intensity of the signal. Similarly, adduct compounds were observed with 2,5-dibromobenzoic acid ($[1 + \mathbf{D}]^+$ at m/z 1005), 3,5-dichlorobenzoic acid ($[1 + \mathbf{E}]^+$ at m/z 916), 4-methoxybenzoic acid ($[1 + \mathbf{F}]^+$ at m/z 877), 2-naphtic acid ($[1 + \mathbf{H}]^+$ at m/z 897) and mandelic acid ($[1 + \mathbf{I}]^+$ at m/z 877), respectively.

2.2. Structural studies

To gain further insight in the binding mode of **1** with monocarboxylic acid, we attempted to crystallise $[1][\text{BF}_4]$ with the same series of monocarboxylic acids. In most cases no crystalline compounds were obtained. However, with 4-bromobenzoic acid, 3,5-dichlorobenzoic acid, 4-methoxybenzoic acid, and 2-naphtic acid, crystals containing a guest molecule were isolated. Crystallographic details are summarised in Table 1. The crystal structure of **1** with benzoic acid has been reported previously [7].

The crystallisation of $[1][\text{BF}_4]$ with 4-bromobenzoic acid (4- $\text{BrC}_6\text{H}_4\text{COOH}$) in an acetone solution gives the host–guest complex $[1][\text{BF}_4] \cdot 4\text{-BrC}_6\text{H}_4\text{COOH}$. The phenyl ring acts as a guest molecule inside the hydrophobic pocket, while the carboxylic acid function interacts with a μ_3 -oxo ligand of a second cluster cation, thus giving rise to a head-to-tail host–guest chain. The

atoms numbering scheme of $[4\text{-BrC}_6\text{H}_4\text{COOHCl}]^+$ is presented in Fig. 2.

The geometry and packing arrangement in the crystal is very similar to the one observed for $[\text{C}_6\text{H}_5\text{COOH}\subset 1][\text{BF}_4]$ [7]. The *p*-bromobenzoic acid, like the benzoic acid molecule, is incorporated inside the hydrophobic pocket. The phenyl ring interacts weakly with the host molecule only by hydrophobic and van der Waals contacts. The angle formed by the C_6 plane and the Ru_3 plane is $82.03(7)^\circ$, the guest molecule being held almost upright in the hydrophobic pocket. On the other hand, the acid function allows the guest molecule to form hydrogen bonds. Indeed, in the solid state, a strong hydrogen bond with the μ_3 -oxo ligand is observed. The $\text{O}\cdots\text{O}$ distance is $2.541(3)$ Å with an $\text{O}\text{--H}\cdots\text{O}$ angle of 167.7° , thus forming a host–guest–host infinite one-dimensional chain, see Fig. 3.

In the crystals obtained with 3,5-dichlorobenzoic acid (3,5- $\text{Cl}_2\text{C}_6\text{H}_3\text{COOH}$), no guest molecule was observed in the hydrophobic pocket of the cluster cation **1**. Instead, a methyl group of symmetry related neighbouring cluster cation is directed in the hydrophobic pocket of **1**. The distance between the methyl carbon and the Ru_3 plane is $3.991(9)$ Å. The atoms numbering scheme of $[1]^+ \cdot 3,5\text{-Cl}_2\text{C}_6\text{H}_3\text{COOH}$ is presented in Fig. 4.

As expected, the acid function forms a hydrogen bond with a μ_3 -oxo ligand. The $\text{O}\cdots\text{O}$ distance is $2.499(9)$ Å with an $\text{O}\text{--H}\cdots\text{O}$ angle of 157.6° . The carbonyl group of the acid function interacts with a chloroform molecule, the $\text{C}\cdots\text{O}$ distance is $3.21(2)$ Å with a $\text{C}\text{--H}\cdots\text{O}$ angle of 155.1° . In the crystal, two independent slipped-parallel π -stacking interactions are observed, one involving the phenyl ring of the $\text{Cl}_2\text{C}_6\text{H}_3\text{COOH}$ and a hexamethyl benzene ligand

Table 1

Crystallographic and selected experimental data for $[\mathbf{1}][\text{BF}_4] \cdot 4\text{-BrC}_6\text{H}_4\text{COOH}$, $[\mathbf{1}][\text{BF}_4] \cdot 3,5\text{-Cl}_2\text{C}_6\text{H}_3\text{COOH} \cdot \text{acetone} \cdot \text{CHCl}_3$, $[\mathbf{1}][\text{BF}_4] \cdot 24\text{-MeOC}_6\text{H}_4\text{COOH} \cdot \text{acetone}$, and $[\mathbf{1}][\text{BF}_4] \cdot 2\text{-C}_{10}\text{H}_7\text{COOH}$

	$[\mathbf{1}][\text{BF}_4] \cdot 4\text{-BrC}_6\text{H}_4\text{COOH}$	$[\mathbf{1}][\text{BF}_4] \cdot 3,5\text{-Cl}_2\text{C}_6\text{H}_3\text{COOH} \cdot \text{acetone} \cdot \text{CHCl}_3$	$[\mathbf{1}][\text{BF}_4] \cdot 24\text{-MeOC}_6\text{H}_4\text{COOH} \cdot \text{acetone}$	$[\mathbf{1}][\text{BF}_4] \cdot 2\text{-C}_{10}\text{H}_7\text{COOH}$
Chemical formula	$\text{C}_{37}\text{H}_{50}\text{BrF}_4\text{O}_3\text{Ru}_3$	$\text{C}_{41}\text{H}_{56}\text{BCl}_5\text{F}_4\text{O}_4\text{Ru}_3$	$\text{C}_{49}\text{H}_{67}\text{BF}_4\text{O}_8\text{Ru}_3$	$\text{C}_{38}\text{H}_{52}\text{BF}_4\text{O}_3\text{Ru}_3$
Formula weight	1012.70	1180.13	923.80	946.82
Crystal system	Monoclinic	Triclinic	Triclinic	Monoclinic
Space group	Cc	$P\bar{1}$	$P\bar{1}$	$C2/c$
Crystal colour and shape	Red block	Red block	Orange block	Red block
Crystal size	$0.33 \times 0.29 \times 0.18$	$0.23 \times 0.18 \times 0.12$	$0.35 \times 0.25 \times 0.12$	$0.22 \times 0.19 \times 0.11$
a (Å)	17.369(2)	10.692(4)	10.9909(15)	31.811(6)
b (Å)	13.9097(17)	13.967(5)	14.377(2)	10.781(2)
c (Å)	16.185(2)	15.785(5)	15.945(2)	23.007(4)
α (°)	90	100.691(5)	101.403(3)	90
β (°)	103.845(2)	96.146(6)	96.800(3)	102.392(3)
γ (°)	90	91.403(6)	93.614(3)	90
V (Å ³)	3796.7(8)	2300.6(14)	2442.7(6)	7706(2)
Z	4	2	2	8
T (K)	100(2)	173(2)	173(2)	100(2)
D_c (g·cm ⁻³)	1.772	1.704	1.596	1.632
μ (mm ⁻¹)	2.285	1.318	0.982	1.215
Scan range (°)	$3.80 < 2\theta < 57.10$	$2.64 < 2\theta < 56.84$	$2.62 < 2\theta < 57.12$	$2.62 < 2\theta < 57.30$
Unique reflections	8834	10500	9997	9342
Refl. used [$I > 2\sigma(I)$]	8264	6996	4319	5486
R_{int}	0.0558	0.0789	0.0979	0.1183
Final R indices [$I > 2\sigma(I)$]	0.0282, wR_2 0.0540	0.0778, wR_2 0.2218	0.0755, wR_2 0.1574	0.0604, wR_2 0.1289
R indices (all data)	0.0322, wR_2 0.0555	0.1153, wR_2 0.2512	0.1830, wR_2 0.2234	0.1254, wR_2 0.1513
Goodness-of-fit	1.023	1.073	0.881	1.009
Max, Min $\Delta\rho/e$ (Å ⁻³)	0.714, -0.481	6.034, -1.836	1.319, -1.436	1.579, -0.993

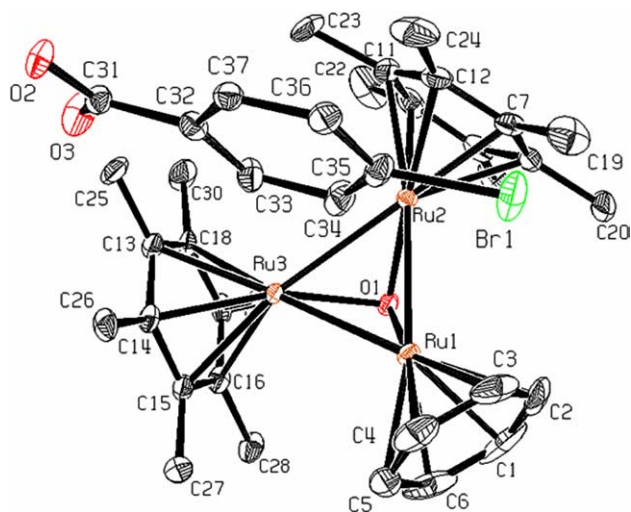


Fig. 2. ORTEP drawing of $[4\text{-BrC}_6\text{H}_4\text{COOH} \cdot \mathbf{1}]^+$, displacement ellipsoids are drawn at the 50% probability level, hydrogen atoms and tetrafluoroborate molecule are omitted for clarity.

(centroid...centroid 3.92 Å), the second between two symmetry related hexamethyl benzene ligand of $\mathbf{1}$ (centroid...centroid 4.11 Å). These interactions are summarised in Fig. 5. The distance observed between the π -stacking interacting systems are slightly longer than the theoretical value calculated for these stacking modes [10].

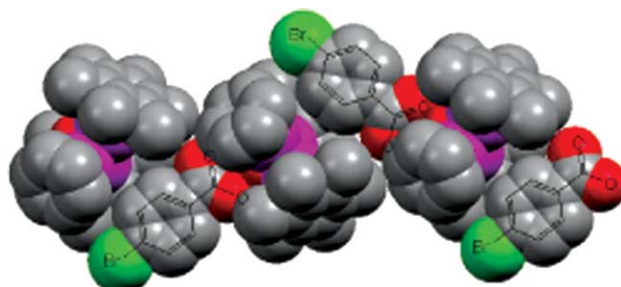


Fig. 3. Infinite host-guest chain of $[4\text{-BrC}_6\text{H}_4\text{COOH} \cdot \mathbf{1}]^+$.

Surprisingly, addition of 4-methoxybenzoic acid ($4\text{-MeOC}_6\text{H}_4\text{COOH}$) to an acetone solution of $[\mathbf{1}][\text{BF}_4]$ gives rise to the formation of $[\mathbf{1}][\text{BF}_4] \cdot 24\text{-MeOC}_6\text{H}_4\text{COOH} \cdot \text{acetone}$, in which one $4\text{-MeOC}_6\text{H}_4\text{COOH}$ participates in a hydrogen bond with the μ_3 -oxo ligand, whereas the second $4\text{-MeOC}_6\text{H}_4\text{COOH}$ forms a dimer with a symmetry related $4\text{-MeOC}_6\text{H}_4\text{COOH}$ molecule, see Fig. 6. As observed in the crystal structure of $[\mathbf{1}][\text{BF}_4] \cdot 3,5\text{-Cl}_2\text{C}_6\text{H}_3\text{COOH}$, a methyl group of a neighbouring cluster molecule is slightly incorporated in the hydrophobic pocket. The distance between the methyl carbon and the Ru_3 plane is 3.96(1) Å.

Finally, with 2-naphtioic acid ($2\text{-C}_{10}\text{H}_7\text{COOH}$), the μ_3 -oxo ligand is also hydrogen-bonded to the acid

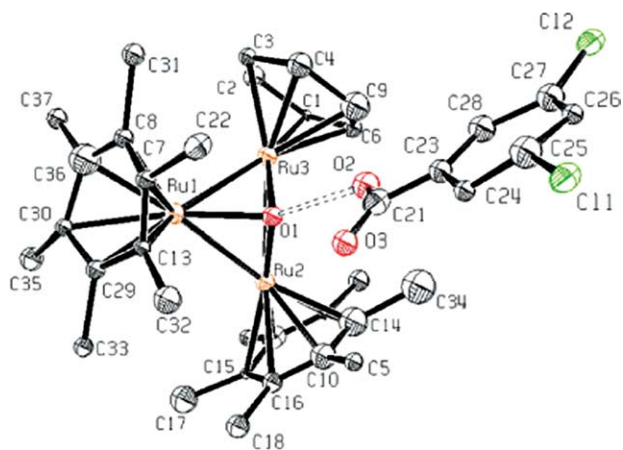


Fig. 4. ORTEP drawing of $[1][BF_4] \cdot 3,5\text{-Cl}_2\text{C}_6\text{H}_3\text{COOH} \cdot \text{CHCl}_3 \cdot \text{acetone}$, displacement ellipsoids are drawn at the 50% probability level, hydrogen atoms, solvent molecules and tetrafluoroborate are omitted for clarity.

function, $\text{O} \cdots \text{O}$ distance 2.583(7) Å, $\text{O}-\text{H} \cdots \text{O}$ angle of 161.1°, see Fig. 7.

Interestingly, the 2-naphtic acid is nested between four cluster molecules, see Fig. 8. The end of the 2-naphtic acid, opposite to the acid function, pointed in the hydrophobic pocket of a cluster cation, the closest carbon–carbon distance being 3.660(9) Å. Two closed parallel π -stacking interactions, with carbon–carbon distances as closed as 3.385(9) and 3.440(9) Å, generate a very compact packing within the crystal.

3. Experimental

3.1. General remarks

Solvents (technical grade) and other reagents were purchased (Aldrich, Fluka) and used as received. The starting compound $[\text{H}_3\text{Ru}_3(\text{C}_6\text{H}_6)(\text{C}_6\text{Me}_6)_2(\text{O})][\text{BF}_4]$

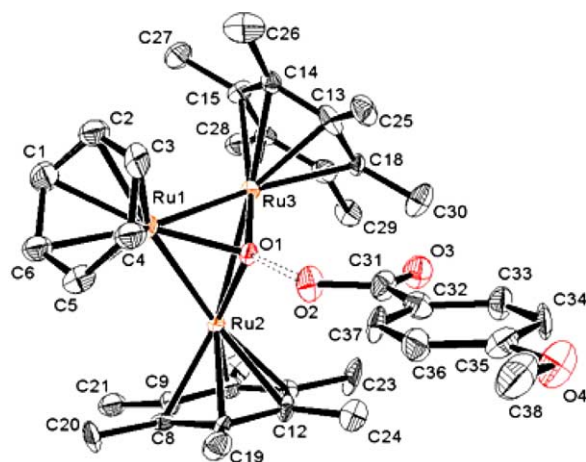


Fig. 6. ORTEP drawing of $[1]^+ \cdot 4\text{-MeOC}_6\text{H}_4\text{COOH}$ (top), dimer of 4-MeOC₆H₄COOH (bottom).

($[1][BF_4]$) was prepared according to published methods [5].

3.2. CSI-MS

Typical measurement conditions are as follows: acceleration voltage, 5.0 kV; needle voltage, 2.9 kV; needle current, 0–1000 nA; orifice voltage, 54 kV; resolution (10% valley definition), 1000; sample flow, 0.5 mL/h; sol-

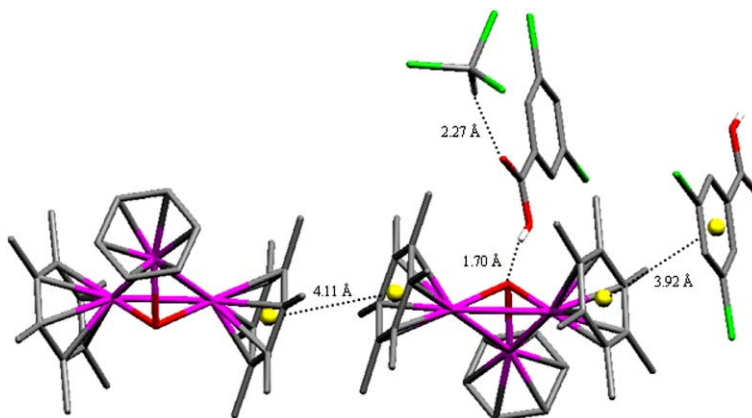


Fig. 5. Main interactions involved in the crystalline packing of $[1][BF_4] \cdot 3,5\text{-Cl}_2\text{C}_6\text{H}_3\text{COOH} \cdot \text{CHCl}_3$.

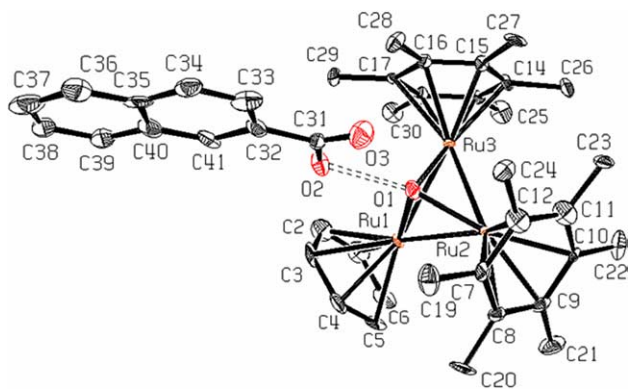


Fig. 7. ORTEP drawing of $[1][BF_4] \cdot 2-C_{10}H_7COOH$, displacement ellipsoids are drawn at the 50% probability level, hydrogen atoms and tetrafluoroborate anion are omitted for clarity.

vent, acetone; spray temperature, $-20\text{ }^\circ\text{C}$; ion source temperature, $25\text{ }^\circ\text{C}$.

3.3. Crystallisations

Preparation of $[1][BF_4] \cdot 4-BrC_6H_4COOH$: In a test tube, 1 mg of $[1][BF_4]$ is added to an acetone solution (3 mL) of $4-BrC_6H_4COOH$ (1 mg). The solution is left at room temperature overnight, the test tube being slightly open, until small red blocks are observed.

Preparation of $[1][BF_4] \cdot 3,5-Cl_2C_6H_3COOH \cdot \text{acetone} \cdot CHCl_3$: In a test tube, 1 mg of $[1][BF_4]$ in acetone is added to a chloroform solution (3 mL) of $3,5-Cl_2C_6H_3COOH$ (1 mg). The solution is left at room tem-

perature for several days, the test tube being slightly open, until thin red blocks are observed.

Preparation of $[1][BF_4] \cdot 24-MeOC_6H_4COOH \cdot \text{acetone}$: In a test tube, 1 mg of $[1][BF_4]$ is added to an acetone solution (3 mL) of $4-MeOC_6H_4COOH$ (1 mg). The solution is left at room temperature for two days, the test tube being slightly open, until orange crystalline blocks are observed.

Preparation of $[1][BF_4] \cdot 2-C_{10}H_7COOH$: To an acetone solution (3 mL) of $[1][BF_4]$ (1 mg) is added 2-naphthoic acid (1 mg). The mixture is left slightly opened overnight, and two days later small red blocks are observed.

3.4. X-ray crystallographic study

The data were measured using a Bruker SMART CCD diffractometer, using Mo $K\alpha$ graphite monochromated radiation ($\lambda = 0.71073\text{ \AA}$). The structures were solved by direct methods using the program SHELXS-97 [11]. The refinement and all further calculations were carried out using SHELXL-97 [12]. The H-atoms were included in calculated positions and treated as riding atoms using the SHELXL default parameters. The non-H atoms were refined anisotropically, using weighted full-matrix least-square on F^2 . In $[1][BF_4] \cdot 2-C_{10}H_7COOH$ the fluor atoms were treated as disordered with partial occupancy factors of 50:50. Figs. 2, 4, 6 and 7 were drawn with ORTEP [13] and Figs. 3, 5 and 8 with MERCURY [14].

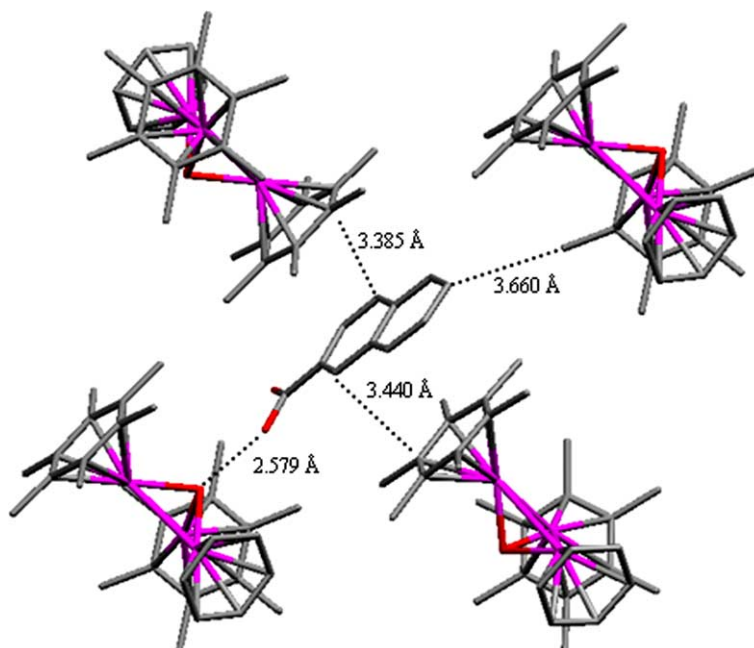


Fig. 8. Naphtoic acid environment in the crystal structure of $[1][BF_4] \cdot 2-C_{10}H_7COOH$.

4. Supplementary data

CCDC-235053 [1][BF₄] \cdot 4-BrC₆H₄COOH, 235054
 [1][BF₄] \cdot 3,5-Cl₂C₆H₃COOH \cdot acetone \cdot CHCl₃, 235055
 [1][BF₄] \cdot 4-MeOC₆H₄COOH \cdot acetone, and 235056
 [1][BF₄] \cdot 2-C₁₀H₇COOH contain the supplementary crystallographic data for this paper. These data can be obtained free of charge via http://www.ccdc.cam.ac.uk/data_request/cif, by emailing data_request@ccdc.cam.ac.uk, or by contacting The Cambridge Crystallographic Data Centre, 12, Union Road, Cambridge CB2 1EZ, UK; fax: +44-1223-336033.

Acknowledgements

This work was supported by the Swiss National Science Foundation (Grant No. 20-67834-02). The authors thank the Johnson Matthey Technology Centre for a generous loan of ruthenium chloride. B. Therrien thanks JSPS, Japan Society for the Promotion of Science, for a fellowship.

References

- [1] (a) M. Kunimura, S. Sakamoto, K. Yamaguchi, *Org. Lett.* 4 (2002) 347;
 (b) S. Sakamoto, K. Nakatani, I. Saito, K. Yamaguchi, *Chem. Commun.* (2003) 788;
 (c) S. Sakamoto, K. Yamaguchi, *Angew. Chem. Intl. Ed. Engl.* 42 (2003) 905;
 (d) K. Yamaguchi, *J. Mass Spectrom.* 38 (2003) 473.
- [2] (a) F. Ibukuro, M. Fujita, K. Yamaguchi, J.-P. Sauvage, *J. Am. Chem. Soc.* 121 (1999) 11014;
 (b) S. Sakamoto, M. Yoshizawa, T. Kusukawa, M. Fujita, K. Yamaguchi, *Org. Lett.* 3 (2001) 1601;
 (c) Y. Yamanoi, Y. Sakamoto, T. Kusukawa, M. Fujita, S. Sakamoto, K. Yamaguchi, *J. Am. Chem. Soc.* 123 (2001) 980;
 (d) S. Sakamoto, T. Imamoto, K. Yamaguchi, *Org. Lett.* 3 (2001) 1793.
- [3] T. Suzuki, Y. Yamagiwa, Y. Matsuo, S. Sakamoto, K. Yamaguchi, M. Shibasaki, R. Noyori, *Tetrahedron Lett.* 42 (2001) 4669.
- [4] (a) S. Sakamoto, M. Fujita, K. Kim, K. Yamaguchi, *Tetrahedron* 56 (2000) 955;
 (b) A. Tsuda, T. Nakamura, S. Sakamoto, K. Yamaguchi, A. Osuka, *Angew. Chem. Intl. Ed. Engl.* 41 (2002) 2817;
 (c) M. Ikeda, M. Takeuchi, S. Shinkai, F. Tani, Y. Naruta, S. Sakamoto, K. Yamaguchi, *Chem. Eur. J.* 8 (2002) 5541;
 (d) M. Ochiai, T. Suefuji, K. Miyamoto, N. Tada, S. Goto, M. Shiro, S. Sakamoto, K. Yamaguchi, *J. Am. Chem. Soc.* 125 (2003) 769.
- [5] M. Faure, M. Jahncke, A. Neels, H. Stoeckli-Evans, G. Süss-Fink, *Polyhedron* 18 (1999) 2679.
- [6] L. Vieille-Petit, B. Therrien, G. Süss-Fink, T.R. Ward, *J. Organomet. Chem.* 684 (2003) 117.
- [7] B. Therrien, L. Vieille-Petit, G. Süss-Fink, *Inorg. Chim. Acta*, in press.
- [8] G. Süss-Fink, M. Faure, T.R. Ward, *Angew. Chem.* 114 (2002) 105;
Angew. Chem. Intl. Ed. 41 (2002) 99.
- [9] NMR conditions; 3.3 mg of benzoic acid, 20 mg of **1** in 0.7 mL of acetone-D₆, Bruker 400 MHz spectrometer, -20 °C.
- [10] S. Tsuzuki, K. Honda, T. Uchimura, M. Mikami, K. Tanabe, *J. Am. Chem. Soc.* 124 (2002) 104.
- [11] G.M. Sheldrick, *SHELXS-97-Program for crystal structure solution*, University of Göttingen, Göttingen, Germany, 1997.
- [12] G.M. Sheldrick, *SHELXL-97-Program for crystal structure refinement*, University of Göttingen, Göttingen, Germany, 1997.
- [13] L.J. Farrugia, *J. Appl. Cryst.* 30 (1997) 565.
- [14] I.J. Bruno, J.C. Cole, P.R. Edgington, M. Kessler, C.F. Macrae, P. McCabe, J. Pearson, R. Taylor, *Acta Cryst.* B58 (2002) 389.